PHYSICS AND CHEMISTRY OF SOLID STATE
V. 27, No. 2 (2026) pp. 382-390
Section: Physics

DOI: 10.15330/pcss.27.2.382-390

Vasyl Stefanyk Carpathian National University

ФІЗИКА І ХІМІЯ ТВЕРДОГО ТІЛА
Т. 27, № 2 (2026) С. 382-390
Фізико-математичні науки

PACS: 78.20.Ci

ISSN 1729-4428 (Print)
ISSN 2309-8589 (Online)

P. Naresh[1], N. Narasimha Rao[2], G. Praveen Chand[3], Babavali Sk. Fakruddin [1], E. Rekha[4]

Photosensitive studies on V_2O_5 doped (40-x)Li_2O-10Y_2O_3-50SiO_2 glasses

[1]*Department of Physics, Velagapudi Ramakrishna Siddhartha School of Engineering, Siddhartha Academy of Higher Education (Deemed to be University), Vijayawada, AP, India, nareshp6@rediffmail.com;*
[2]*Department of Physics, Krishna University Dr.MRAR College of PG Studies, Nuzvid, AP, India;*
[3]*Department of Chemistry, RVR & JC College of Engineering (Autonomous), Chowdavaram, Guntur, AP, India;*
[4]*Government Degree College, Pakala, Chittoor Dist., AP, India*

In this study, glass systems with chemical composition (40-x)Li_2O–10Y_2O_3–50SiO_2:xV_2O_5 were prepared using melt-quenching method. The XRD patterns of the prepared samples conform to the glassy nature. Optical absorption spectra exhibit two absorption bands at around roughly 630 nm and 1030 nm, identified as the transitions due to $^2B_2 \rightarrow {}^2B_1$ and $^2B_2 \rightarrow {}^2E$ transitions of $[VO]^{2+}$ ions. The intensities of these identified peaks are observed to grow with a slightly red shift with the V_2O_5 content in the glass matrix. The direct and indirect optical band gaps, evaluated using Davis-Mott theory, decreased with increasing V_2O_5 concentration, while the Urbach energy obtained from the Urbach rule increased. IR spectral analysis revealed that the glass samples exhibit various structural units via., $Si-O-Si$ asymmetric and symmetric stretching $Si-O-Y$ linkages, $V=O$, $Si-O-V$ linkages and $Li-O$; it appeared that the intensity of asymmetric linkages was observed to increase by the expense of symmetric linkages with a gradual increase in the content of V_2O_5. The optical absorption spectra of the investigated glasses suggest the coexistence of V^{4+} and V^{5+} ionic species. The observed evolution of the characteristic vanadyl absorption bands with increasing V_2O_5 concentration indicates a possible shift in the V^{4+}/V^{5+} equilibrium within the glass network.

Keywords: Optical Absorption, FTIR, alkali mixed glasses, silicate glasses.

Received 14 May 2025; Accepted 25 June 2026; Published 30 June 2026.

Introduction

Alkali silicate glasses like lithium silicate glasses exhibit remarkable thermal stability, enhanced ion changeability, exceptional chemical durability, optical transparency over electric wavelength, and compositional dependent tunable refractive index rendering them particularly advantageous for ion exchange glasses like phone screens, photovoltaic cells, short distance data busses. When certain sesquioxide (e.g., Sb_2O_3, Al_2O_3, Y_2O_3, La_2O_3, Sc_2O_3, etc.,) are combined with alkali silicate glasses, their optical/ luminescence, mechanical, electrical, chemical and thermal - physical properties will be enhanced significantly with composition [1-12]. When Y_2O_3 is added to the alkali-silicate glass systems, it broadness the spectral transparency, improves the refractive index, and decreases phonon energies [8-10].

Yttrium oxide is a sesquioxide, when it used as an additive in glass admixture, helps to improve various properties like physical, chemical, optical, and thermal properties. The concentration of yttrium particularly in silicate glasses changes the durability by changing the network connectivity by the broader range of atomic environments [11]. Yttrium can act as a network modifier or former, as first one it breaks the network and reduces the number of non-bridging oxygens (NBOs) [12], as later one it forms bonds with oxygen and contributes to the rigidity of the glass network [13]. The literature study [14-21] strongly proved that properties like hardness, elastic modulus, glass stability, thermal expansion coefficient, and sealing behavior were enhanced by the yttrium ions in the various glass compositions.

A vanadate-based glass exhibits desirable properties with tunable features such as good electrical conductivities from insulating to semi-conducting range, chemical durability in aggressive mediums like acids, and bases and also possesses low crystallization tendency during solidification [22-30]. Because of these characteristics; vanadate glasses could be used in cathode materials for solid-state devices and optical fibers as well as in electrical threshold, threshold switching, memory switching, and optical switching devices [31-37]. V_2O_5 is mentioned as a conditional glass former since it rapidly forms glass only when combined with a modifier, such as an alkali, alkaline earth, transition metal oxides (TMOs), or another glass former [25, 38-40].

Vanadium ions exist in glass matrix in two distinct valence states, V^{4+} and V^{5+}, thus vanadate glasses are categorized as amorphous oxide semiconductors [41]. A 3d1 unpaired electron migrating from a V^{4+} site to a V^{5+} site causes lattice polarization, which in turn produces a polaron, which is the phenomena known as electrical conductivity [42-46].

In the present paper, we have synthesized (40-x)Li_2O–10Y_2O_3–50SiO_2: xV_2O_5 and the structural modifications that occur as a result of the diverse oxidation states of vanadium ions, as examined through optical absorption and infrared spectral analyses which were very important for the selection of material for various above-mentioned applications such as optical fibers, modulators, electrodes in solid-state batteries.

I. Materials and Methods

The flow chart illustrating the procedure adopted for the preparation of the glass samples is presented in Figure 1. The detailed methodology used for sample preparation is similar to that reported in our previous studies [47, 48]. The compositional details of the investigated glass samples are presented in Table 1. Details of the instruments used for obtaining the experimental data are presented in Table 2.

Table 1.

Compositional details (all in mol %)

Sample code	Composition in mol%
$LYSV_0$	40.0 Li_2O–10Y_2O_3–50SiO_2
$LYSV_2$	39.8 Li_2O–10Y_2O_3–50SiO_2: 0.2 V_2O_5
$LYSV_4$	39.6 Li_2O–10Y_2O_3–50SiO2: 0.4 V_2O_5
$LYSV_6$	39.4 Li_2O–10Y_2O_3–50SiO_2: 0.6 V_2O_5
$LYSV_8$	39.2 Li_2O–10Y_2O_3–50SiO_2: 0.8 V_2O_5
$LYSV_{10}$	39.0 Li_2O–10Y_2O_3–50SiO_2: 1.0 V_2O_5

Table 2.

Details of the instruments

Study	Details of the instrument used
XRD	Xpert PRO diffractometer
UV-Vis absorption	JASCO Model V-670 UV-Vis-NIR spectrometer
IR Transmission spectra	JASCO-FT/IR-5300 spectrophotometer by utilizing 300 mg of KBr pellets containing ground up material

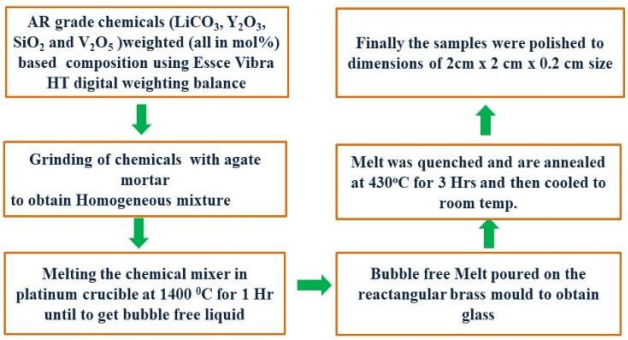

Fig. 1. Flow chart of various steps involved in preparation of (40-x)Li_2O−10Y_2O_3− 50SiO_2: xV_2O_5 glass samples.

II. Results and Discussion

Figure 2 displays XRD patterns of (40-x)Li_2O–10Y_2O_3–50SiO_2:xV_2O_5 samples. It indicates that there are no distinct sharp peaks in the XRD patterns of the prepared samples, revealing that the materials possess an amorphous nature.

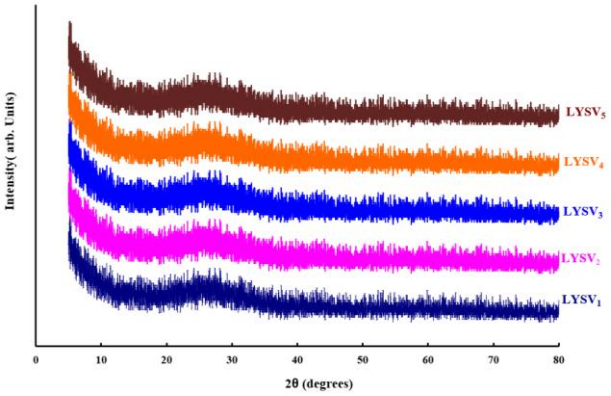

Fig. 2. XRD Patterns of (40-x)Li_2O-10Y_2O_3-50SiO_2: xV_2O_5 glass samples.

Figure 3 (a) illustrates the optical absorption spectra (OA) of (40-x)Li_2O–10Y_2O_3–50SiO_2:xV_2O_5 glasses. For pure glass ($LYSV_0$) the absorption edge is found at 340 nm and when the concentration of V_2O_5 increases, it is seen to progressively shift towards higher wavelengths. Furthermore, two absorption bands at 650 nm and 1080 nm which correspond to $^2B_2 \rightarrow {}^2B_1$ and $^2B_2 \rightarrow {}^2E$ transitions of VO^{2+} ions were visible in the spectra of glasses doped with 0.2 mol% of V_2O_5 [49];

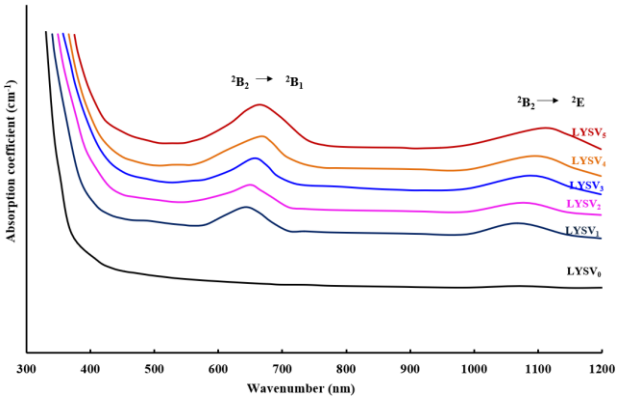

Fig. 3(a). Optical absorption spectra of (40-x)Li_2O-10Y_2O_3-50SiO_2: xV_2O_5 glass samples.

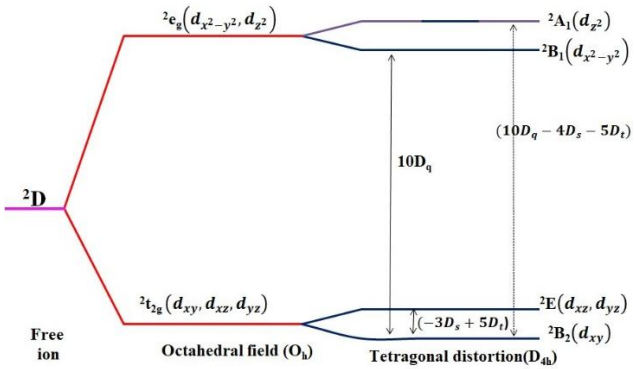

Fig. 3(b). Schematic energy levels of V^{4+} in an octahedral field with tetragonal distortion.

Vanadium is a transition metal placed in group 5 with ground state electronic configuration [Ar]$3d^34s^2$. Among $3d^34s^2$ valence electrons, 3d electrons play a dynamic role in vanadium chemical behavior due to existence in multiple oxidation states. Hence vanadium ions likely to be exist primarily in the V^{5+} state in the vanadium-doped lithium yttrium silicate glasses. However, during melting, and annealing it might be undergone equilibrium redox reaction as follows [50]:

$$2V^{5+} + O^{2-} \longrightarrow 2\,V^{4+} + \frac{1}{2}O_2 \uparrow$$

Here the d^1 configuration of the V^{4+} ion has ^2D as its ground state. The ^2D state splits into $^2t_{2g}$ ($|d_{xy}\rangle, |d_{xz}\rangle, |d_{yz}\rangle$) and ^2e_g ($|d_{x^2-y^2}\rangle, |d_{z^2}\rangle$) when a pure octahedral crystal field is present, while the $^2t_{2g}$ level further splits into ^2E_g (double degenerate, $|d_{xz}\rangle, |d_{yz}\rangle$) and $^2B_2$ (non-degenerate, $|d_{xy}\rangle$) when an octahedral field with tetragonal distortion (compression/elongation along the z-axis) is present; the $^2B_2$ state will be the ground state of these. Additionally ^2e_g level splits into $^2A_1|d_{z^2}\rangle$ and $^2B_1|d_{x^2-y^2}\rangle$. The schematic energy levels for V^{4+} ion in the octahedral field with tetragonal distortion are shown in Fig 3(b). Therefore, for the vanadyl ions, we can anticipate three bands corresponding to transitions $^2B_2 \rightarrow {}^2B_1$ ($d_{xy} \rightarrow d_{x^2-y^2}$), $^2B_2 \rightarrow {}^2E$ ($d_{xy} \rightarrow d_{xz,yz}$) and $^2B_2 \rightarrow {}^2A_1$ ($d_{xy} \rightarrow d_{z^2}$) [51].

However, only the first two bands are visible in the present investigated glasses, this might be due to multiple reasons like the same spin multiplicity, parity forbidden same d→d transition and weaker intensity of degree of distortion. The appearance of these absorption bands, commonly attributed to the $^2B_2 \rightarrow {}^2B_1$ and $^2B_2 \rightarrow {}^2E$ transitions of VO^{2+} species reported in the literature [49, 51], provides indirect spectroscopic evidence for the presence of V^{4+} ions in the investigated glass samples. In addition, the half-width and peak height of these bands are observed to increase and shift towards a somewhat higher wavelength as the concentration of V_2O_5 is increased up to 1.0 mol %. The octahedral crystal field splitting parameters (D_q) and tetragonal crystal field parameters (D_s and D_t) satisfy the standard relations:

$$^2B_2 - {}^2B_1 = 10D_q$$

$$^2B_2 - {}^2E = -3D_s + 5D_t$$

$$^2B_2 - {}^2A_1 = 10D_q - 4D_s - 5D_t$$

Table 3 shows the D_q values that were evaluated from $^2B_2 - {}^2B_1$ transition that was observed with an increase in V_2O_5 content. The details of the cut-off wavelengths and the corresponding band positions were also presented in Table 3.

It should be noted that the oxidation state assignment presented in this work is based on optical spectroscopic signatures reported in the literature. Therefore, the conclusions regarding the coexistence of V^{4+} and V^{5+} species should be considered qualitative rather than quantitative. A definitive determination of the V^{4+}/V^{5+} ratio would require complementary techniques such as ESR or EPR etc.

According to Davis and Mott's theory [52, 53], the optical edge of non-crystalline materials can be expressed by the equation:

$$\alpha h\vartheta = A\left(h\vartheta - E_{opt}\right)^r$$

Where α, absorption coefficient, A proportionality constant, hν, photon energy, E_{opt}, optical band gap energy, r = 2(allowed indirect), ½ (allowed direct), 3 (forbidden indirect), and 1/3 (forbidden direct) transitions respectively. The direct and indirect optical band gaps

Table 3.

Data on Optical absorption spectra of $(40\text{-}x)Li_2O–10Y_2O_3–50SiO_2$: xV_2O_5 Glass samples

Sample		$LYSV_0$	$LYSV_1$	$LYSV_2$	$LYSV_3$	$LYSV_4$	$LYSV_5$
Conc. of V_2O_5	mol%	0	0.2	0.4	0.6	0.8	1.0
Cutoff wavelength, nm		330	340	351	357	366	375
Band position , nm	$^2B_2 \rightarrow {}^2B_1$	---	642	649	655	665	668
	$^2B_2 \rightarrow {}^2E$	---	1068	1077	1081	1099	1104
Crystal field splitting parameter Dq, (cm^{-1})			1158	1141	1127	1504	1497
Optical band gap, eV	r =2	3.38	3.12	2.94	2.84	2.78	2.70
	r =3	3.42	3.18	3.4	2.92	2.86	2.76
	r =1/2	2.72	2.58	2.48	2.40	2.36	2.28
	r =1/3	2.42	1.88	1.80	1.68	1.46	1.40
Urbach Energy, eV		0.40	0.60	0.81	0.95	0.91	1.13

were estimated by extrapolations of the $(\alpha h\vartheta)^r vs\ h\vartheta$ curves at $(\alpha h\vartheta)^r = 0$. Plots of $(\alpha h\vartheta)^r vs\ h\vartheta$ as a function of energy along with the extrapolations for the (40-x)Li_2O-10Y_2O_3-50SiO_2: x V_2O_5 glasses (x= 0 -1.0 mol%) are systematically presented in Fig. 4 (a-d). The estimated direct, indirect allowed as well as forbidden energy bands are presented in Table 3 showing a decrease in the value of the band gap (both direct and indirect) E_g with the increase in the concentration of V_2O_5.

In amorphous oxide glasses, the absence of long-range periodicity results in the formation of localized electronic states near the band edges, commonly referred to as band-tail states. Consequently, the optical absorption process cannot always be described by a single transition mechanism. Within the Davis-Mott's formalism, different values of the exponent 'r' are employed to investigate various possible electronic transitions occurring between extended and localized states. The allowed direct and allowed indirect transition models are generally associated with the fundamental absorption processes and provide estimates of the mobility gap of the glass. In contrast, the forbidden direct and forbidden indirect transition models are particularly sensitive to localized defect states, structural imperfections, and disorder-induced electronic levels within the amorphous network. Therefore, the simultaneous analysis of all four transition models enables a more comprehensive assessment of the electronic structure, degree of of disorder, and defect-related modifications induced by V_2O_5 incorporation. Furthermore, comparison of the trends obtained from different transitions models provides additional confidence in the observed evolution of the optical band gap and its correlation with structural changes in the glass matrix.

According to the Urbach rule [54], the absorption coefficient (α) near the band edge follows an exponential dependence on photon energy (E):

$$\alpha(E) = \alpha_0 exp\left(\frac{E-E_0}{\Delta E}\right)$$

Where, E_0, characteristic energy; ΔE, Urbach energy; α_0, constant;

The Urbach rule serves as a diagnostic tool for assessing disorder, temperature dependency and electronic transitions in solid-state materials especially disordered ones. Hence, the degree of disorder in prepared glasses was characterized using Urbach energy calculated from the reciprocal slope of the linear portion of band edges of the *ln(α) vs* hν plots. Urbach plots for the current studied glass samples were presented in Figure 4(e). These estimated Urbach energies are presented in Table 3. From these pertained values, it is observed that the Urbach energy increases with the concentration of V_2O_5.

The observed decrease in the optical band gap with a rise in V_2O_5 concentration can be explicated as follows; the excited states of localized electrons that were initially trapped on VO^{2+} sites start to overlap with the vacant 3d states on the nearby V^{5+} sites, as result of increment of vanadyl ion concentration in the glass. As a result, the impurity band consequently extends farther into the main band gap. This change may have caused the absorption edge to move to the lower energy, resulting in notable band gap shrinkage. Whereas, the increase in Urbach energy with an increase in the concentration of V_2O_5, indicates the increase in the degree of disordered-ness in glass samples. Summing the observed increase broadness of the mentioned peaking in the OA spectra and the increase in the Urbach energy suggested that the distribution of energy levels due to the increase in the degree of disorder.

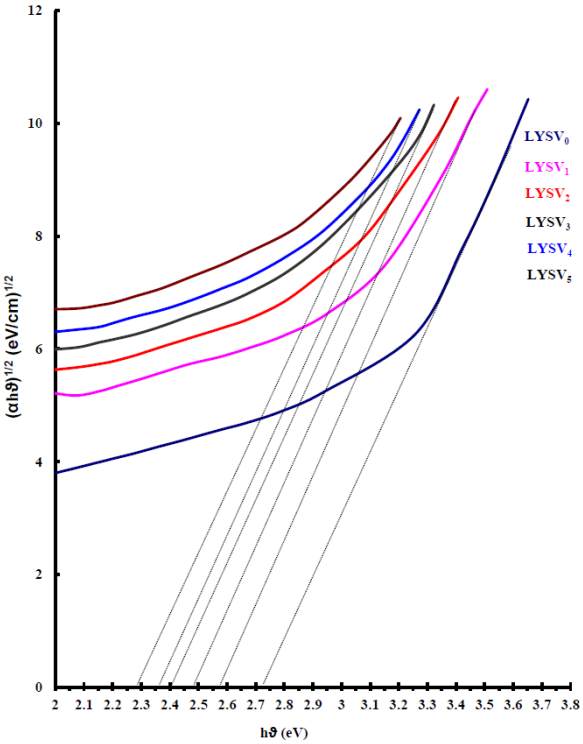

Fig 4(a). $(ahv)^{1/2}$ vs hν plots of (40-x)Li_2O−10Y_2O_3−50SiO_2: xV_2O_5 glass samples.

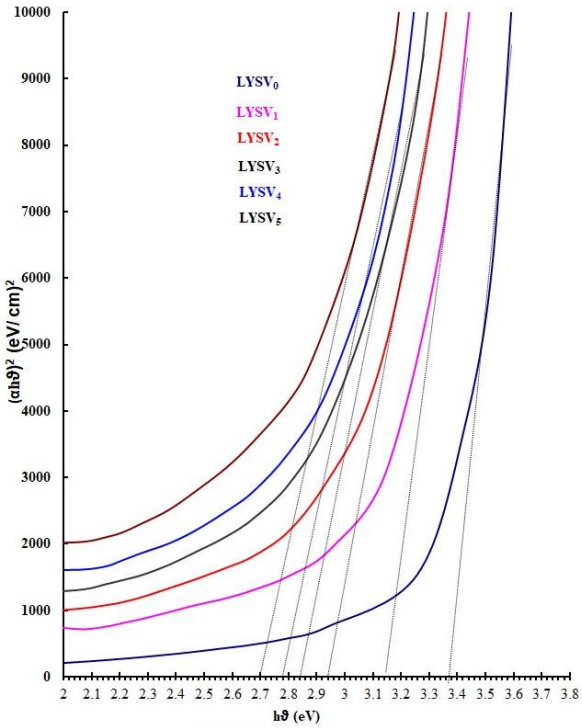

Fig. 4(b). $(ahv)^2$ vs hν plots of (40-x)Li_2O−10Y_2O_3−50SiO_2: xV_2O_5 glass samples.

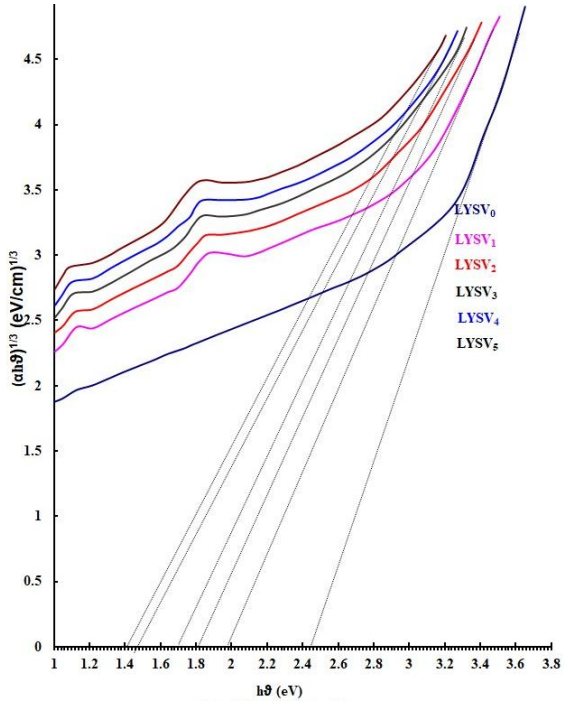

Fig. 4(c). $(ahv)^{1/3}$ vs hv plots of (40-x)Li_2O−10Y_2O_3−50SiO_2: xV_2O_5 glass samples.

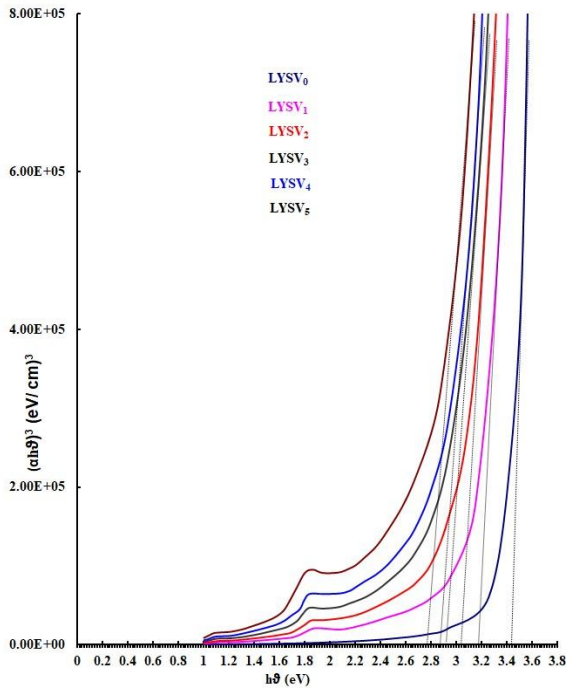

Fig. 4(d). $(ahv)^3$ vs hv plots of (40-x)Li_2O−10Y_2O_3−50SiO_2: xV_2O_5 glass samples.

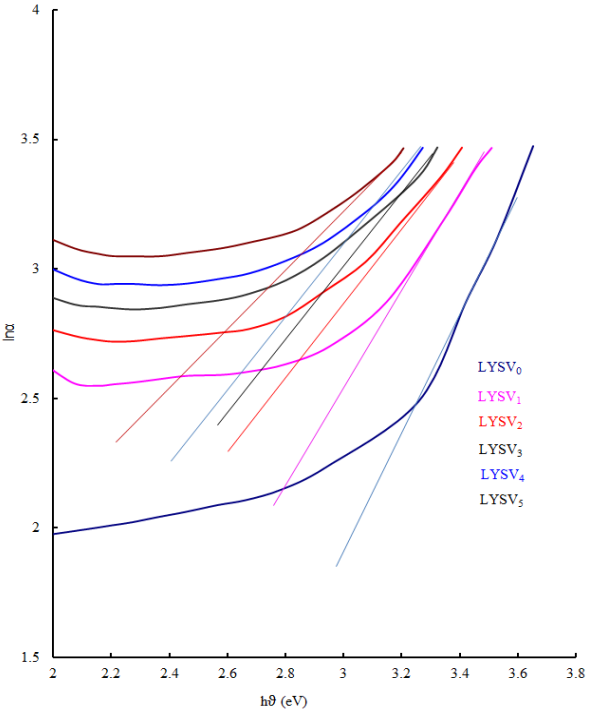

Fig. 4(e). ln$a$ vs hv plots of (40-x)Li_2O−10Y_2O_3−50SiO_2: xV_2O_5 glass samples.

Silica glass is well-known glass former with fundamental structural units of SiO_4 tetrahedral, forming a continuous random network using bridging oxygens. Typically, the bond length of Si−O is 1.6 °A [55]; The O−Si−O bond angle is around 109.5°; Si−O−Si bond angles vary from 120° to 180° with variable tendency due to the amorphous nature as well as leading to flexibility in the network. In pure silica glass, all oxygen atoms are bridging oxygens [56]. However, the introduction of modifiers or impurities can lead to breaking the bonding of oxygen and form NBOs [57]. Figure 5 displays infrared transmission spectra (IR) of Li_2O–Y_2O_3–SiO_2:V_2O_5 glasses. The spectra showed a typical vibrational band caused by Si−O−Si asymmetric vibrations at around 1083 cm^{-1} and Si−O−Si symmetric vibrations at 787 cm^{-1}.

With the addition of Y_2O_3 into SiO_2 glasses, the structure of the SiO_2 alters significantly by acting as a network modifier, disrupting the Si−O−Si network that forms NBOs. With the relatively large size and charge of the Y^{3+} ions, Si^{4+} creates local distortions and increases the free volume within the glass network.

Adding the Li_2O to the Y_2O_3−SiO_2, NBOs as well reduce the viscosity of the glass melt and increases the ionic conductivity due to the small size and high charge density of Li^+ ions. The combined addition of Y_2O_3 and Li_2O can have synergistic effects on the glass structure with enhanced depolymerization compared to the individual effects. By carefully adjusting the ratio of Li_2O-Y_2O_3, it becomes a promising material with tailored material of viscosity, thermal expansion and chemical durability, for specific applications.

These spectra also show the octahedral band of yttrium ions (YO_6) at roughly 482 cm^{-1} [58,59] In this area the band resulting from Si-O-Si rocking motion is also predicted [60, 61]. With the addition of V_2O_5, there is an extra band at 970 cm^{-1} from V–O stretching of the V=O group, a band at 815 cm^{-1} from V−O−V stretching and at 600 cm^{-1} due to V−O−V bending vibrations [62]. The bands seen in the glass V_1 spectrum at 980 cm^{-1} and 800 cm^{-1} may be regarded as typical vibrational modes of Si–O–V stretching. Bands resulting from asymmetrical vibrations of silicate and other structural units are seen to expand at the expense of symmetrical bands as the concentrations of V_2O_5 in the glass samples are progressively increased. Table 4 displays the pertinent information about the infrared transmission spectra of glasses.

Table 4.

Data on Infrared Spectra (40-x)Li_2O–10Y_2O_3–50SiO_2: xV_2O_5 glasses recorded at Room Temperature (Assignment of Band Positions in cm^{-1})

Assignment	$LYSV_0$	$LYSV_2$	$LYSV_4$	$LYSV_6$	$LYSV_8$	$LYSV1_0$
Si–O–Si asymmetric/ Si–O–Y	1079	1065	1057	1050	1043	1034
V=O	--	975	970	967	953	950
Si–O–Si symmetric/V-O-V chains	784	805	821	834	841	851
V-O-V bendings	--	611	604	606	598	590
Si–O–Si rocking motions/ YO_6 units	465	471	463	460	467	469

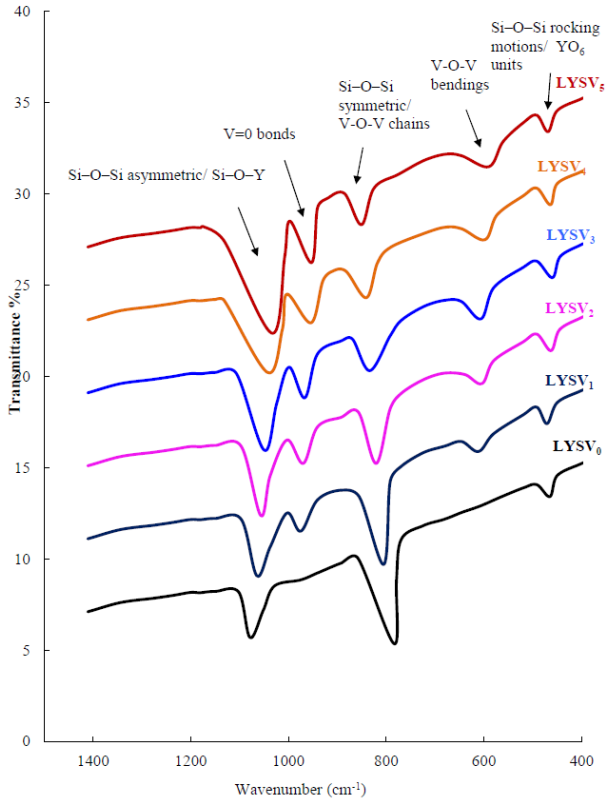

Fig. 5. IR spectra of (40-x)Li_2O-10Y_2O_3-50SiO_2: xV_2O_5 glass samples.

The gradual shift of the Si–O–Si asymmetric stretching vibration towards lower wavenumbers with increasing V_2O_5 concentration indicates modifications in the silicate network. The incorporation of vanadium ions promotes the formation of Si–O–V bonds and generates additional non-bridging oxygen sites, leading to partial depolymerization of the glass network. Such structural rearrangements decrease the average network connectivity and increase the structural disorder of the glass matrix. The appearance and growth of V=O and V–O–V vibrational bands further confirm the participation of vanadium structural units in the glass network. These structural modifications are consistent with the observed reduction in optical band gap and increase in Urbach energy.

Conclusion

(40-x)Li_2O–10Y_2O_3–50SiO_2: xV_2O_5 (x =0, 0.2, 0.4, 0.6, 0.8 &1.0) were successfully prepared using the melt–quenching technique. The XRD analysis confirmed the amorphous nature of the glass samples. The broad absorption bands observed in the optical absorption spectra were assigned to $^2B_2 \rightarrow {}^2B_1$ and $^2B_2 \rightarrow {}^2E$ transitions of $[VO^{2+}]$ ions in an octahedral field with tetragonal distortion. The octahedral crystal-field splitting parameter (D_q) was evaluated. Based on Davis and Mott's theory, allowed direct, allowed indirect optical band gaps were primarily analyzed, while forbidden direct, and forbidden indirect optical band gaps were additionally examined to gain insight into localized electronic states associated with structural disorder. The optical band gaps values were found to decrease, whereas the Urbach energy increased with increasing V_2O_5 concentration. This behaviour indicates an increase in structural disorder and the formation of localized states within the glass network upon V_2O_5 incorporation.

FTIR spectral analysis revealed the presence of various structural units involving Si–O–Si, Si–O–Y, Si–O–V, V=O, and V–O–V linkages; the asymmetric vibrational bands were observed to broaden at the expense of the corresponding symmetric bands with increasing V_2O_5 concentration. Analysis of the optical absorption and FTIR spectra suggests the coexistence of V^{4+} and V^{5+} ionic species in the investigated glasses. The evolution of the characteristic vanadyl absorption bands with increasing V_2O_5 concentration indicates possible changes in the V^{4+}/V^{5+} equilibrium.

Naresh P. – Ph.D, Assistant Professor (SG), Department of Physics, VR Siddhartha School of Engineering, Siddhartha Academy of Higher Education (Deemed to be University), Vijayawada, Andhra Pradesh, India;
Narasimha Rao N. – Ph.D, Assistant Professor, Department of Physics, Krishna University Dr.MRAR College of PG Studies, Nuzvid, AP, India;
Praveen Chand G. – Ph. D, Assistant Professor, Department of Chemistry, RVR & JC College of Engineering (Autonomous), Chowdavaram, Guntur-522019, Andhrapradesh, India;
Fakruddin Babavali Sk. – Ph.D, Assistant Professor (SG), Department of Physics, VR Siddhartha School of Engineering, Siddhartha Academy of Higher Education (Deemed to be University), Vijayawada, Andhra Pradesh, India;
Rekha E. – Ph.D, lecture in physics, Government degree College, Pakala, Chittor Dist., AP, India.

[1] A.O.G. Dikovska, P.A. Atanasov, M. Jiménez de Castro, A. Perea, J. Gonzalo, C.N. Afonso and J. García-López, *Optically active Er^{3+}–Yb^{3+} co-doped Y_2O_3 films produced by pulsed laser deposition*, Thin Solid Films, 500(1), 336 (2006); https://doi.org/10.1016/j.tsf.2005.11.022.

[2] I. Alekseeva, O. Dymshits, M. Tsenter and A. Zhilin, *Influence of various alkali* and divalent metal oxides on phase transformations in NiO-doped glasses of the Li_2O–Al_2O_3–SiO_2–TiO_2 system, Journal of Non-Crystalline Solids, 357(11-13), 2209 (2011); https://doi.org/10.1016/j.jnoncrysol.2010.12.065.

[3] M.A. Hughes, T. Suzuki and Y. Ohishi, *Compositional optimization of bismuth-doped yttria–alumina–silica glass*, Optical Materials, 32(2), 368 (2009); https://doi.org/10.1016/j.optmat.2009.09.004.

[4] J. Kong, D.Y. Tang, B. Zhao, J. Lu, K. Ueda, H. Yagi and T. Yanagitani, *9.2-W diode-end-pumped Yb ceramic laser*, Applied Physics Letters, 86(16), 161116 (2005); https://doi.org/10.1063/1.1914958.

[5] M.T. Tokurakawa, K. Shimura, A. Ueda, K. Yagi, H. Yagi, T. Kamimura and A. Ikesue, *Diode-pumped 188 fs mode-locked Yb^{3+} ceramic laser*, Applied Physics Letters, 90(7), 071101 (2007); https://doi.org/10.1063/1.2476385.

[6] H. Guo, W. Zhang, L. Lou, A. Brioude and J. Mugnier, *Structure and optical properties of rare earth doped Y_2O_3 waveguide films derived by sol–gel process*, Thin Solid Films, 458(1), 274 (2004); https://doi.org/10.1016/j.tsf.2003.12.059.

[7] M.B. Korzenski, P. Lecoeur, B. Mercey, P. Camy and J.L. Doualan, *Low propagation losses of an Er planar waveguide grown by alternate-target pulsed laser deposition,* Applied Physics Letters, 78(9), 1210 (2001); https://doi.org/10.1063/1.1347026.

[8] C. Srinivasa Rao, I.V. Kityk, T. Srikumar, G. Naga Raju, V. Ravi Kumar, Y. Gandhi and N. Veeraiah, *Spectroscopy features of Pr^{3+} and Er^{3+} ions in Li_2O–ZrO_2–SiO_2 glass matrices mixed with some sesquioxides,* Journal of Alloys and Compounds, 509(37), 9230 (2011); https://doi.org/10.1016/j.jallcom.2011.07.001.

[9] G. K. Marasinghe et al., Redox *Characteristics and Structural Properties of Iron Phosphate Glasses: A Potential Host Matrix for Vitrifying High Level Nuclear Waste*, Ceramic Transactions, 87, 261 (1998).

[10] P. Venkateswara Rao, M. Srinivasa Reddy, K.S.V. Sudhakar and N. Veeraiah, *Influence of iron ions on dielectric properties of the PbO–Bi_2O_3–B_2O_3 glass system*, Philosophical Magazine, 88(11), 1601 (2008); https://doi.org/10.1080/14786430802238386.

[11] A. Moguš-Milanković, L. Pavić, K. Srilatha, C. Srinivasa Rao, T. Srikumar, Y. Gandhi and N. Veeraiah, *Electrical, dielectric and spectroscopic studies on MnO doped LiI–AgI–B_2O_3 glasses*, Journal of Applied Physics, 111(1), 013714 (2012); https://doi.org/10.1063/1.3676254.

[12] S.M. Salem, E.K.A. Khalek, E.A. Mohamed and M. Farouk, *A study on the optical, structural, electrical conductivity and dielectric properties of lithium bismuth germanium tungsten glasses*, Journal of Alloys and Compounds, 513, 35 (2012); https://doi.org/10.1016/j.jallcom.2011.09.052.

[13] J.K. Christie and A. Tilocca, *Aluminosilicate glasses as yttrium vectors for in situ radiotherapy: understanding composition-durability effects through molecular dynamics simulations*, Chemistry of Materials, 22(12), 3725 (2010); https://doi.org/10.1021/cm100847p.

[14] X. Li et al., *Topological models of yttrium aluminosilicate glass based on molecular dynamics and structure characterization analysis*, Journal of the American Ceramic Society, 108(1), e20118 (2025); https://doi.org/10.1111/jace.20118.

[15] K.S. Habana, A.M. Al-Baradi, Z.A. Alrowaili et al., *Structural, thermal, and mechanical characteristics of yttrium lithium borate glasses and glass–ceramics*, Journal of Materials Science: Materials in Electronics, 32, 28065 (2021); https://doi.org/10.1007/s10854-021-07158-w.

[16] A. Arafat et al., *Thermal and crystallization kinetics of yttrium-doped phosphate-based glasses*, International Journal of Applied Glass Science, 11(1), 120 (2020); https://doi.org/10.1111/ijag.14163.

[17] E.A. Mahdy and S. Ibrahim, *Influence of Y_2O_3 on the structure and properties of calcium magnesium aluminosilicate glasses,* Journal of Molecular Structure, 1027, 81 (2012); https://doi.org/10.1016/j.molstruc.2012.05.055.

[18] M.S. Shakeri and M. Rezvani, *Optical band gap and spectroscopic study of lithium alumino silicate glass containing Y^{3+} ions*, Spectrochimica Acta Part A: Molecular and Biomolecular Spectroscopy, 79(5), 1920 (2011); https://doi.org/10.1016/j.saa.2011.05.090.

[19] D.S. Brauer et al., *Effect of TiO_2 addition on structure, solubility and crystallisation of phosphate invert glasses for biomedical applications*, Journal of Non-Crystalline Solids, 356(44-49), 2626 (2010); https://doi.org/10.1016/j.jnoncrysol.2010.03.022.

[20] I.H. Arita, D.S. Wilkinson and G.R. Purdy, *Crystallization of yttria–alumina–silica glasses*, Journal of the American Ceramic Society, 75(12), 3315 (1992); https://doi.org/10.1111/j.1151-2916.1992.tb04427.x.

[21] V. Kumar, O.P. Pandey and K. Singh, *Thermal and crystallization kinetics of yttrium and lanthanum calcium silicate glass sealants for solid oxide fuel cells*, International Journal of Hydrogen Energy, 36(22), 14971 (2011); https://doi.org/10.1016/j.ijhydene.2011.05.124.

[22] R.A. Montani and M.A. Frechero, *Mixed ion-polaron transport in lithium vanadium–molybdenum tellurite glasses*, Solid State Ionics, 177(33), 2911 (2006); https://doi.org/10.1016/j.ssi.2006.08.015.

[23] M. Prashant Kumar and T. Sankarappa, *DC conductivity in some alkali doped vanadotellurite glasses*, Solid State Ionics, 178(33), 1719 (2008); https://doi.org/10.1016/j.ssi.2007.11.003.

[24] C.N. Reddy, V.C. Veeranna Gowda and R.P. Sreekanth Chakradhar, *Elastic properties and structural studies on lead–boro–vanadate glasses*, Journal of Non-Crystalline Solids, 354(1), 32 (2008); https://doi.org/10.1016/j.jnoncrysol.2007.07.011.
[25] Y.B. Saddeek, E.R. Shaaban, K.A. Aly and I.M. Sayed, *Characterization of some lead vanadate glasses,* Journal of Alloys and Compounds, 478(1), 447 (2009); https://doi.org/10.1016/j.jallcom.2008.11.063.
[26] G.D. Khattak, A. Mekki and L.E. Wenger, *X-ray photoelectron spectroscopy (XPS) and magnetic susceptibility studies of vanadium phosphate glasses*, Journal of Non-Crystalline Solids, 355(43), 2148 (2009); https://doi.org/10.1016/j.jnoncrysol.2009.06.042.
[27] L. Murawski, *AC conductivity in binary V_2O_5–P_2O_5 glasses*, Philosophical Magazine B, 50(6), 69 (1984); https://doi.org/10.1080/13642818408238888.
[28] E.R. Shaaban, M.Y. Hassaan, A.G. Mostafa and A.M. Abdel-Ghany, *Crystallization kinetics of new compound of V_2O_5–PbO–Li_2O–Fe_2O_3 glass using differential thermal analysis*, Journal of Alloys and Compounds, 482(1), 440 (2009); https://doi.org/10.1016/j.jallcom.2009.04.062.
[29] C. Narayana Reddy and R.V. Anavekar, *Elastic properties and spectroscopic studies of Li_2O–B_2O_3–V_2O_5 glasses,* Materials Chemistry and Physics, 112(2), 359 (2008); https://doi.org/10.1016/j.matchemphys.2008.05.062.
[30] M.M. El-Desoky, *Characterization and transport properties of V_2O_5–Fe_2O_3–TeO_2 glasses*, Journal of Non-Crystalline Solids, 351(37), 3139 (2005); https://doi.org/10.1016/j.jnoncrysol.2005.08.004.
[31] S.R. Ovshinsky, *Reversible electrical switching phenomena in disordered structures*, Physical Review Letters, 21(20), 1450 (1968); https://doi.org/10.1103/PhysRevLett.21.1450.
[32] C.F. Drake, I.F. Scanlon and A. Engel, *Electrical switching phenomena in transition metal glasses under the influence of high electric fields,* Physica Status Solidi A, 32(1), 193 (1969); https://doi.org/10.1002/pssb.19690320121.
[33] J. Livage, J.P. Jollivet and E. Tronc, *Electronic properties of mixed valence oxide gels*, Journal of Non-Crystalline Solids, 121(1-3), 35 (1990); https://doi.org/10.1016/0022-3093(90)90100-Z.
[34] R. Balaji Rao, N.O. Gopal and N. Veeraiah, *Studies on the influence of V_2O_5 on dielectric relaxation and AC conduction phenomena of Li_2O–MgO–B_2O_3 glass system*, Journal of Alloys and Compounds, 368(1), 25 (2004); https://doi.org/10.1016/j.jallcom.2003.08.077.
[35] P. Pascuta, G. Borodi and E. Culea, *Influence of europium ions on structure and crystallization properties of bismuth borate glasses and glass ceramics*, Journal of Non-Crystalline Solids, 354(52), 5475 (2008); https://doi.org/10.1016/j.jnoncrysol.2008.09.010.
[36] R.A. Montani, M. Levy and J.L. Souquet, *An electrothermal model for high-field conduction and switching phenomena in TeO_2–V_2O_5 glasses*, Journal of Non-Crystalline Solids, 149(3), 249 (1992); https://doi.org/10.1016/0022-3093(92)90073-S.
[37] A. Ghosh and B.K. Chaudhuri, *Anomalous conductivity and other properties of V_2O_5–P_2O_5 glasses with Bi_2O_3 or Sb_2O_3*, Journal of Non-Crystalline Solids, 103(1), 83 (1988); https://doi.org/10.1016/0022-3093(88)90419-X.
[38] K. Singh, J. Ratnam and V.K. Deshpande, *The influence of V_2O_5 on the electrical conductivity of Li_2O–B_2O_3 system*, Solid State Ionics, 28-30, 821 (1988); https://doi.org/10.1016/S0167-2738(88)80154-1.
[39] G. Chiodelli, A. Magistris, M. Villa and J.L. Bjorkstam, *Structure and ion dynamics in AgI–$Ag_2B_4O_7$ vitreous electrolytes*, Materials Research Bulletin, 17(1), 1 (1982); https://doi.org/10.1016/0025-5408(82)90176-3.
[40] V.C. Veeranna Gowda and R.V. Anavekar, *Elastic properties* and spectroscopic studies of lithium lead borate glasses, Ionics, 10(1-2), 103 (2004); https://doi.org/10.1007/BF02410315.
[41] D. Maniu, T. Iliescu and S. Astilean, Raman study of lead vanadate glasses, Romanian Reports in Physics, 56(3), 419 (2004).
[42] M. Sayer and A. Mansingh, *Transport properties of semiconducting phosphate glasses*, Physical Review B, 6(12), 4629 (1972); https://doi.org/10.1103/PhysRevB.6.4629.
[43] N.F. Mott, *Conduction in glasses containing transition metal ions*, Journal of Non-Crystalline Solids, 1(1), 1 (1968); https://doi.org/10.1016/0022-3093(68)90002-1.
[44] I.G. Austin and N.F. Mott, *Polarons in crystalline and non-crystalline materials*, Advances in Physics, 18(71), 41 (1969); https://doi.org/10.1080/00018736900101267.
[45] C.H. Chung and J.D. Mackenzie, *Electrical properties of binary semiconducting oxide glasses containing 55 mole% V_2O_5*, Journal of Non-Crystalline Solids, 42(1-3), 357 (1980); https://doi.org/10.1016/0022-3093(80)90036-8.
[46] A.E. Owen, *The electrical properties of glasses*, Journal of Non-Crystalline Solids, 25(1-3), 351 (1977); https://doi.org/10.1016/0022-3093(77)90099-0.
[47] P. Naresh et al., *Optical studies of chromium doped zinc oxy fluoro borate glasses – A possible disordered material for tunable lasers*, Materials Today: Proceedings, 46, 806 (2021); https://doi.org/10.1016/j.matpr.2020.12.769.
[48] N. Narasimha Rao et al., *Vanadium oxides impact on the ZnO–Sb_2O_3–B_2O_3 glasses dielectric and AC conduction mechanisms*, International Journal of Mathematics and Physics, 15(1), 91 (2024); https://doi.org/10.26577/ijmph.2024v15i1a11.
[49] J. Ballhausen and H.B. Gray, *The electronic structure of the vanadyl ion*, Inorganic Chemistry, 1(1), 111 (1962); https://doi.org/10.1021/IC50001A022.

[50] S. Bahammam, S. Abd and F.M. Ezz-Eldin, *Synthesis and characterization of γ-irradiated cadmium-borate glasses doped with V_2O_5,* Results in Physics, 7, 241 (2017); https://doi.org/10.1016/j.rinp.2016.12.042.
[51] R. Lakshmikantha, N.H. Ayachit and R.V. Anavekar, *Optical, physical and structural studies of vanadium doped P_2O_5–BaO–Li_2O glasses*, Journal of Physics and Chemistry of Solids, 75(2), 168 (2014); https://doi.org/10.1016/j.jpcs.2013.09.004.
[52] E.A. Davis and N.F. Mott, *Conduction in non-crystalline systems V. Conductivity, optical absorption and photoconductivity in amorphous semiconductors*, Philosophical Magazine, 22(179), 903 (1970); https://doi.org/10.1080/14786437008221061.
[53] J. Tauc (Ed.), Amorphous and Liquid Semiconductors (Springer Science & Business Media, New York, 2012).
[54] F. Urbach, *The long-wavelength edge of photographic sensitivity and of the electronic absorption of solids*, Physical Review, 92, 1324 (1953); https://doi.org/10.1103/PhysRev.92.1324.
[55] E. Görlich, *The structure of SiO_2—Current views*, Ceramics International, 8(1), 3 (1982); https://doi.org/10.1016/0272-8842(82)90009-8.
[56] D.L. Griscom, *Optical properties and structure of defects in silica glass*, Journal of the Ceramic Society of Japan, 99(1154), 923 (1991); https://doi.org/10.2109/jcersj.99.923.
[57] H. Jabraoui et al., *Effect of sodium oxide modifier on structural and elastic properties of silicate glass*, The Journal of Physical Chemistry B, 120(51), 13193 (2016) https://doi.org/10.1039/C7CP03397D.
[58] Y. Qian and H. Gao, *Upconversion properties of Y_2O_3 films prepared by sol–gel method*, Journal of Rare Earths, 27(3), 406 (2009); https://doi.org/10.1016/S1002-0721(08)60261-6.
[59] H. Liang, Y. Zheng, G. Chen, L. Wu, Z. Zhang and W. Cao, *Enhancement of up-conversion luminescence of Y2O3+ nanocrystals by co-doping Li^+–Zn^{2+}*, Journal of Alloys and Compounds, 509(2), 409 (2011); https://doi.org/10.1016/j.jallcom.2010.09.044.
[60] K.J. Rao, Structural Chemistry of Glasses (Elsevier, Amsterdam, 2002).
[61] M. Nakamura, Y. Mochizuki, K. Usami, Y. Itoh and T. Nozaki, *Infrared absorption spectra and compositions of evaporated silicon oxides (SiO_x),* Solid State Communications, 50(12), 1079 (1984); https://doi.org/10.1016/0038-1098(84)90292-8.
[62] K. Tanaka, K. Kamiya and T. Yoko, *ESR and Mössbauer studies of Bi_2O_3–Fe_2O_3 glasses*, Journal of Non-Crystalline Solids, 109(2-3), 289 (1989); https://doi.org/10.1016/0022-3093(89)90042-2.

П. Нареш[1], Рао Н. Нарасімха[2], Чанд Г. Правін[3], Бабавалі Ск. Факруддін[1], Е. Рекха[4]

Фоточутливі дослідження стекол (40-x)Li_2O–$10Y_2O_3$–$50SiO_2$, легованих V_2O_5

[1] *Кафедра фізики, Інженерна школа Велагапуді Рамакрішни Сіддхартхи, Академія Сіддхартхи (університет зі статусом deemed to be university), Віджаявада, Андхра-Прадеш, Індія, nareshp6@rediffmail.com;*
[2] *Кафедра фізики, Університет Крішни, Коледж післядипломної освіти Dr. MRAR, Нузвід, Андхра-Прадеш, Індія;*
[3] *Кафедра хімії, Інженерний коледж RVR & JC (автономний), Чоудаварам, Гунтур, Андхра-Прадеш, Індія;*
[4] *Державний коледж, Пакала, округ Чіттур, Андхра-Прадеш, Індія*

У дослідженні скляні системи хімічного складу (40-x)Li_2O–$10Y_2O_3$–$50SiO_2$:xV_2O_5 були отримані методом плавлення з наступним загартуванням. Рентгенодифракційні (XRD) дослідження підтвердили аморфну природу синтезованих зразків. Спектри оптичного поглинання демонструють дві смуги поглинання приблизно при 630 нм та 1030 нм, які ідентифіковано як переходи $^2B_2 \rightarrow {}^2B_1$ та $^2B_2 \rightarrow {}^2E$ іонів $[VO]^{2+}$ відповідно. Інтенсивність цих смуг зростає та супроводжується незначним червоним зміщенням зі збільшенням вмісту V_2O_5 у скляній матриці. Пряма та непряма оптичні ширини забороненої зони, визначені за теорією Девіса–Мотта, зменшуються зі зростанням концентрації V_2O_5, тоді як енергія Урбаха, розрахована за правилом Урбаха, збільшується. Аналіз ІЧ-спектрів показав наявність у зразках різних структурних одиниць, зокрема асиметричних та симетричних валентних коливань Si–O–Si, зв'язків Si–O–Y, V=O, Si–O–V та Li–O. Встановлено, що інтенсивність асиметричних зв'язків зростає за рахунок симетричних зі збільшенням вмісту V_2O_5. Спектри оптичного поглинання досліджуваних стекол свідчать про співіснування іонних станів V^{4+} та V^{5+}. Спостережувана еволюція характерних смуг поглинання ванадилу зі збільшенням концентрації V_2O_5 вказує на можливе зміщення рівноваги V^{4+}/V^{5+} у скляному середовищі.

Ключові слова: оптичне поглинання, FTIR, змішані лужні стекла, силікатні стекла.